

DTP/98/12  
March 1998

## Diffractive dijet photoproduction as a probe of the off-diagonal gluon distribution

K. Golec-Biernat<sup>1</sup>, J. Kwiecinski<sup>1</sup>, and A.D. Martin  
Department of Physics, University of Durham, DH1 3LE, UK

### Abstract

We propose exclusive diffractive dijet photoproduction as an ideal measure of the off-diagonal gluon distribution at high scales. We solve the off-diagonal evolution equations for the gluon and quark singlet over the full kinematic domain. We discuss the nature of the solutions of these equations, which embody both DGLAP and ERBL evolution. We give predictions for the transverse momentum distribution of the jets. In particular we quantify the enhancement arising from the evolution of the off-diagonal parton distributions.

---

<sup>1</sup>On leave from H. Niewodniczanski Institute of Nuclear Physics, Department of Theoretical Physics, ul. Radzikowskiego 152, Krakow, Poland.

# 1 Introduction

Traditionally diffractive processes are described, within perturbative QCD, by two gluon exchange [1]. An example is the  $\gamma p \rightarrow q\bar{q}p$  process sketched in Fig. 1, where the outgoing  $q\bar{q}$  system may emerge either as a vector meson or as two jets. It has been argued that the amplitudes for these reactions are proportional to the conventional gluon distribution<sup>2</sup>  $G(x_{IP}) \equiv x_{IP}g(x_{IP})$ , with  $x_{IP}$  given by

$$x_{IP} = \frac{M^2 + Q^2}{W^2 + Q^2}, \quad (1)$$

where  $M$  is the invariant mass of the diffractive  $q\bar{q}$  system and  $W$  is the  $\gamma p$  centre-of-mass energy. The variable  $x_{IP}$  is the fraction of the proton longitudinal momentum transferred to the diffractive system by the exchange of the two gluons. A non-zero virtuality of the photon,  $Q^2 \neq 0$ , allows electroproduction processes to be considered, in addition to photoproduction with  $Q^2 = 0$ .

We notice that the two exchanged gluons in Fig. 1 carry different momentum fractions  $x$  and  $x'$ , and so the process should actually be described by an off-diagonal gluon distribution  $G(x, x')$ . For vector meson electro- or photo-production it turns out that it is a good approximation to use the off-diagonal distribution  $G(x_{IP}, 0)$  with  $x = x_{IP}$  and  $x' = 0$ . The error made in using the traditional diagonal distribution  $G(x_{IP}, x_{IP}) = x_{IP}g(x_{IP})$  has been quantified in Ref. [2] (related work can be found in [3]). There the DGLAP-type evolution equation for the off-diagonal distribution  $G(x, x')$  was solved and compared with standard DGLAP evolution for  $xg(x)$ . The ratio

$$R(x, x') = \frac{G(x, x')}{xg(x)} \quad (2)$$

was calculated as a function of  $Q^2$ , for different choices of (diagonal) starting distributions. The ratio  $R(x, x')$  was, as expected, found to be above unity and to increase with  $Q^2$  and with  $x_{IP} \equiv x - x'$ . For example the off-diagonal effects for  $J/\psi$  photoproduction can be estimated from the values obtained for  $R$  at  $x = x_{IP}$  and  $x' = 0$ . From Ref. [2] we see that the  $J/\psi$  amplitude is enhanced by  $R(x, 0) \simeq 1.1$  by off-diagonal evolution. The prediction for the cross section is thus increased by a factor of about 1.2.

Ref. [2] considered only the off-diagonal effects arising from DGLAP-type evolution and so the analysis was restricted to the domain  $x' \geq 0$ . The difference with the conventional diagonal distribution was found to be largest when  $x' = 0$  and to decrease rapidly with increasing  $x'$ . That is  $R(x, x')$  was largest when  $x' = 0$  and rapidly decreased to unity as  $x' \rightarrow x$ . However the DGLAP domain is only a part of a more general evolution of the off-diagonal distribution. In the region  $x' < 0$  the gluon  $G(x, x')$  looks like the distribution *amplitude* for the proton to *emit* two gluons and consequently obeys an ERBL-type evolution equation [4, 5]. Therefore processes which depend on a wider range of  $x'$ , and in particular sample the  $x' < 0$  region, may be subject to much larger off-diagonal effects than the  $J/\psi$  example that we mentioned above.

One such process is the exclusive diffractive production of a pair of (quark) jets with high values of transverse momenta  $\pm \mathbf{p}_T$ . For this process it is necessary to work in terms of the off-diagonal gluon distribution  $f$  unintegrated over the transverse momentum of the gluon,

$$f(x, x', k_T^2) = \frac{\partial G(x, x', k_T^2)}{\partial \ln k_T^2}. \quad (3)$$

---

<sup>2</sup>The scale at which the gluon distribution is evaluated is  $z(1-z)Q^2 + p_T^2 + m_q^2$ , where  $m_q$  and  $\pm \mathbf{p}_T$  are the mass and transverse momenta of the emitted quarks, and  $z$  is the fraction of photon momentum carried by one of the quarks. So perturbative QCD is valid if either  $Q^2$  (with  $z \sim 1/2$ ),  $p_T^2$  or  $m_q^2$  is large.

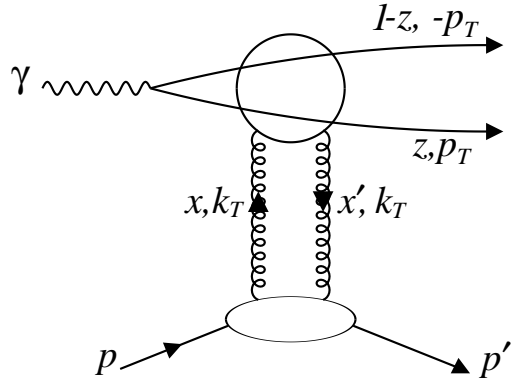


Figure 1: The QCD subprocess  $\gamma p \rightarrow (q\bar{q})p'$ , describing the exclusive diffractive photoproduction of dijets.

The computation of the high  $p_T$  dijet production cross section requires integration over the entire region of  $k_T$  (with an important contribution coming from the region  $k_T \sim p_T$ ). Hence this process explores the detailed properties of the off-diagonal gluon distribution (3) in a broad range of  $x'$  and  $k_T$ . In fact we will find that an important contribution comes from the region  $|x'| \sim x_{IP}$  which should be compared to  $x' = 0$  which is relevant for diffractive  $J/\psi$  production. As a result we are able to study the much richer structure of the full evolution equations, which combine DGLAP-like as well as ERBL-like features.

The content of the paper is as follows. In Section 2 we present the formula for the diffractive dijet cross section driven by the off-diagonal unintegrated gluon distribution. We carefully examine the kinematic relations relevant for the off-diagonal analysis. In Section 3 we present a simplified analysis which provides valuable insight into the process, as well as forming the basis for a comparison with our full off-diagonal treatment. The kinematic relations relevant to the perturbative and nonperturbative regions are given in Section 4. Then in Section 5 we study in detail the full evolution equations of the off-diagonal distributions, which embody both DGLAP and ERBL components. The detailed form of these equations is given in the Appendix. The effect of using the off-diagonal distributions to predict the cross section for the exclusive diffractive dijet photoproduction is quantified in Section 6. Finally Section 7 contains a brief summary of our main results.

## 2 General form of the diffractive dijet cross section

The differential cross sections for the exclusive diffractive production of dijets from transversely and longitudinally polarised photons, described by the QCD subprocess  $\gamma^* p \rightarrow (q\bar{q})p'$  shown in Fig. 1, have the structure (see also [6])

$$\frac{d\sigma_{T,L}}{d^2\mathbf{p}_T dt} \Big|_{t=0} = \frac{\alpha\alpha_S^2}{6\pi} \sum_q e_q^2 \int_0^1 dz \int \frac{d^2\mathbf{k}_T}{k_T^4} \frac{d^2\bar{\mathbf{k}}_T}{\bar{k}_T^4} \tilde{f}(x, x', k_T^2) \tilde{f}(\bar{x}, \bar{x}', \bar{k}_T^2) \Phi_{T,L}^q(z, \mathbf{k}_T, \bar{\mathbf{k}}_T, \mathbf{p}_T), \quad (4)$$

where  $\pm \mathbf{p}_T$  are the transverse momenta of the quark jets,  $z$  and  $(1-z)$  are their longitudinal momentum fractions and the barred variables refer to the amplitude which is the complex conjugate of the amplitude of the process shown in Fig. 1. Formula (4) was obtained assuming that the imaginary part of the amplitude dominates, with the neglect of a possible contribution from the real part. To compute the imaginary part we have to take into account the four possible

ways that the two exchanged gluons can couple to the two quarks forming the dijet system. This is reflected both in the structure of the impact factors  $\Phi_{T,L}^q$  and in the gluon distribution function  $\tilde{f}$ . Strictly speaking the notation for the arguments of  $\tilde{f}$  is symbolic and is only meant to indicate that we are dealing with two gluons with different longitudinal momentum fractions  $x$  and  $x'$ . To be precise  $\tilde{f}$  is the following linear combination of the off-diagonal distributions (3)

$$\tilde{f}(x, x', k_T^2) = \frac{1}{2} \left[ f(x(x'), x', k_T^2) + f(x(x''), x'', k_T^2) \right], \quad (5)$$

where

$$x(x') = x_{IP} + x' \quad \text{and} \quad x(x'') = x_{IP} + x'', \quad (6)$$

are equal to the longitudinal momentum fractions carried by the first gluon (the gluon emitted from the proton in Fig. 1). The variables  $x'$  and  $x''$  are the longitudinal momentum fractions of the second gluon according to whether it couples to the quark with the momentum fraction  $z$  and  $(1 - z)$  respectively. That is

$$x' = \frac{k_T^2 + 2\mathbf{p}_T \cdot \mathbf{k}_T}{z(Q^2 + W^2)} \quad \text{and} \quad x'' = \frac{k_T^2 + 2\mathbf{p}_T \cdot \mathbf{k}_T}{(1 - z)(Q^2 + W^2)}. \quad (7)$$

For the complex conjugate amplitudes we have analogous formulae for  $\bar{x}'$  and  $\bar{x}''$  with  $\mathbf{k}_T$  replaced by  $\bar{\mathbf{k}}_T$ . The first gluon momentum fractions are always *positive* whereas the second gluon fractions  $x'$  and  $x''$  can be *negative* for  $k_T < 2p_T$ . In this case the second gluon is emitted, rather than absorbed as is shown in Fig. 1. Notice also that  $x_{IP}$ , defined by (1) with a diffractive mass of the dijet system given by

$$M^2 = \frac{p_T^2 + m_q^2}{z(1 - z)}, \quad (8)$$

plays the role of the asymmetry variable  $\zeta \equiv x - x' = x_{IP}$  for our process.

Finally, the impact factors  $\Phi_T^q$  and  $\Phi_L^q$  are [6]

$$\Phi_T^q(z, \mathbf{k}_T, \bar{\mathbf{k}}_T, \mathbf{p}_T) = [z^2 + (1 - z)^2] \Phi_1(z, \mathbf{k}_T, \bar{\mathbf{k}}_T, \mathbf{p}_T) + m_q^2 \Phi_2(z, \mathbf{k}_T, \bar{\mathbf{k}}_T, \mathbf{p}_T) \quad (9)$$

and

$$\Phi_L^q(z, \mathbf{k}_T, \bar{\mathbf{k}}_T, \mathbf{p}_T) = 4Q^2 z^2 (1 - z)^2 \Phi_2(z, \mathbf{k}_T, \bar{\mathbf{k}}_T, \mathbf{p}_T), \quad (10)$$

where

$$\begin{aligned} \Phi_1(z, \mathbf{k}_T, \bar{\mathbf{k}}_T, \mathbf{p}_T) &= \left\{ \frac{p_T^2}{[p_T^2 + \bar{Q}^2]^2} - \frac{\mathbf{p}_T \cdot (\mathbf{p}_T + \mathbf{k}_T)}{[p_T^2 + \bar{Q}^2][(p_T + \mathbf{k}_T)^2 + \bar{Q}^2]} \right. \\ &\quad \left. - \frac{\mathbf{p}_T \cdot (\mathbf{p}_T + \bar{\mathbf{k}}_T)}{[p_T^2 + \bar{Q}^2][(p_T + \bar{\mathbf{k}}_T)^2 + \bar{Q}^2]} + \frac{(\mathbf{p}_T + \mathbf{k}_T) \cdot (\mathbf{p}_T + \bar{\mathbf{k}}_T)}{[(p_T + \mathbf{k}_T)^2 + \bar{Q}^2][(p_T + \bar{\mathbf{k}}_T)^2 + \bar{Q}^2]} \right\}, \end{aligned} \quad (11)$$

and

$$\begin{aligned} \Phi_2(z, \mathbf{k}_T, \bar{\mathbf{k}}_T, \mathbf{p}_T) &= \left\{ \frac{1}{[p_T^2 + \bar{Q}^2]^2} - \frac{1}{[p_T^2 + \bar{Q}^2][(p_T + \mathbf{k}_T)^2 + \bar{Q}^2]} \right. \\ &\quad \left. - \frac{1}{[p_T^2 + \bar{Q}^2][(p_T + \bar{\mathbf{k}}_T)^2 + \bar{Q}^2]} + \frac{1}{[(p_T + \mathbf{k}_T)^2 + \bar{Q}^2][(p_T + \bar{\mathbf{k}}_T)^2 + \bar{Q}^2]} \right\}, \end{aligned} \quad (12)$$

with

$$\overline{Q}^2 \equiv z(1-z)Q^2 + m_q^2. \quad (13)$$

Cross section (4) is invariant under the interchange  $z \leftrightarrow (1-z)$ . Thus we may replace the upper limit of the  $z$  integration by  $1/2$  and multiply the final result by 2. Now the upper limit corresponds to the *minimal* value of the pomeron momentum fraction  $x_{\mathcal{P}\min}$  (or diffractive mass  $M^2 = 4(p_T^2 + m_q^2)$ ) necessary to produce a dijet system with jets of transverse momenta  $\pm \mathbf{p}_T$ . The lower limit  $z_{\min}$  corresponds to the *maximal* allowed value of  $x_{\mathcal{P}\max}$  (usually  $x_{\mathcal{P}\max} < 0.1$ ). Thus from (1) and (8) we obtain

$$z_{\min} = \frac{1}{2} \left\{ 1 - \sqrt{1 - \frac{4(p_T^2 + m_q^2)}{x_{\mathcal{P}\max}(Q^2 + W^2) - Q^2}} \right\}. \quad (14)$$

We now study the integrations in (4) with respect to the azimuthal angles  $\phi$  and  $\overline{\phi}$  between the jet transverse momentum  $\mathbf{p}_T$  and the gluon momenta  $\mathbf{k}_T$  and  $\overline{\mathbf{k}}_T$ , respectively. The angular structure of the impact factors  $\Phi_1$  and  $\Phi_2$  allows us to rewrite the cross section formula (4) in the following remarkably compact forms

$$\frac{d\sigma_T}{d^2\mathbf{p}_T dt} \Big|_{t=0} = \frac{\alpha\alpha_S^2}{3\pi p_T^2} \sum_q e_q^2 \int_{z_{\min}}^{1/2} dz \left\{ [z^2 + (1-z)^2] [\phi_1(z, p_T)]^2 + \frac{m_q^2}{p_T^2} [\phi_2(z, p_T)]^2 \right\} \quad (15)$$

and

$$\frac{d\sigma_L}{d^2\mathbf{p}_T dt} \Big|_{t=0} = \frac{\alpha\alpha_S^2}{3\pi p_T^2} \sum_q e_q^2 \int_{z_{\min}}^{1/2} dz \left\{ z^2(1-z)^2 \frac{4Q^2}{p_T^2} [\phi_2(z, p_T)]^2 \right\}, \quad (16)$$

where the new ‘‘impact factors’’  $\phi_1$  and  $\phi_2$  have the following forms

$$\phi_1(z, p_T) = \int \frac{dk_T^2}{k_T^4} \int_0^\pi d\phi \tilde{f}(x, x', k_T^2) \frac{1}{2} \left\{ \frac{1-\omega^2}{1+\omega^2} - \frac{2-a}{a+b\cos\phi} \right\}, \quad (17)$$

$$\phi_2(z, p_T) = \int \frac{dk_T^2}{k_T^4} \int_0^\pi d\phi \tilde{f}(x, x', k_T^2) \left\{ \frac{1}{1+\omega^2} - \frac{1}{a+b\cos\phi} \right\}. \quad (18)$$

For convenience we have introduced the dimensionless quantities

$$\omega = \overline{Q}/p_T, \quad \tau = k_T/p_T, \quad a = 1 + \omega^2 + \tau^2 \quad \text{and} \quad b = 2\tau. \quad (19)$$

The cross section formulae (15) and (16) are quite general. They do not depend on any particular behaviour of the gluon distribution function. The crucial observation to obtain these formulae is that the terms which could spoil the new impact factor factorization are odd with respect to the angles  $\phi$  and  $\overline{\phi}$ . Thus they give a vanishing contribution when the full azimuthal integrations are performed.

### 3 Insight from the simplified case

The angular integrations in (17) and (18) cannot be performed analytically since the arguments  $x$  and  $x'$  of the nonforward gluon distribution  $f$  depend on the angle  $\phi$ . It is illuminating, however,

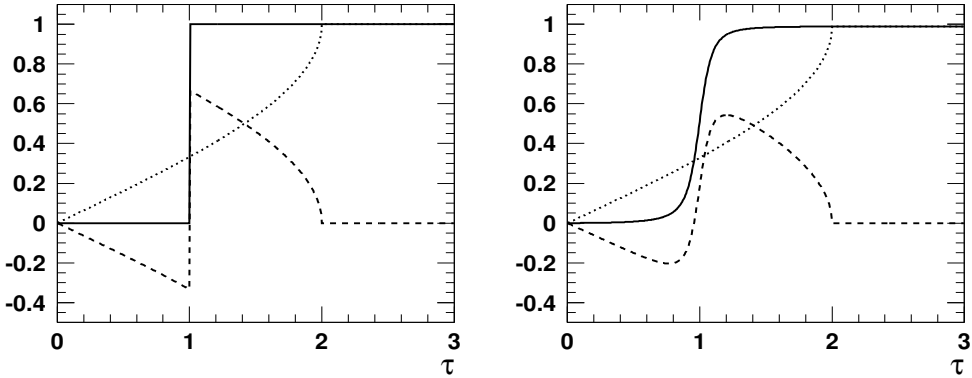


Figure 2: The integrand in the curly brackets in (20) as a function of  $\tau \equiv k_T/p_T$  (solid curves). We also show the contributions from the  $x' > 0$  (dotted curves) and  $x' < 0$  (dashed curves) regions separately. The two figures correspond to  $\omega \equiv \bar{Q}/p_T = 0$  (left) and  $\omega = 0.1$  (right).

to first consider a simplified situation in which  $\tilde{f} = f(x_{IP}, k_T^2)$  depends on  $x_{IP} = x - x'$ , and not on  $x$  and  $x'$  separately. This situation was implicitly assumed in [6]. Then  $f$  is independent of  $\phi$  and the angular integration can be performed, and we obtain

$$\phi_1(z, p_T) = \pi \int \frac{dk_T^2}{k_T^4} f(x_{IP}, k_T^2) \frac{1}{2} \left\{ \frac{1 - \omega^2}{1 + \omega^2} - \frac{2 - a}{\sqrt{a^2 - b^2}} \right\} \quad (20)$$

and

$$\phi_2(z, p_T) = \pi \int \frac{dk_T^2}{k_T^4} f(x_{IP}, k_T^2) \left\{ \frac{1}{1 + \omega^2} - \frac{1}{\sqrt{a^2 - b^2}} \right\}. \quad (21)$$

In the limiting case  $\omega = \bar{Q}/p_T \rightarrow 0$ , which corresponds to diffractive dijet photoproduction with high values of  $p_T$ , the only appreciable contribution to the cross section (15) comes from the  $\phi_1$  term. In this limit  $(2 - a) \rightarrow (1 - \tau^2)$  and  $\sqrt{a^2 - b^2} \rightarrow |1 - \tau^2|$  and so (20) becomes simply

$$\phi_1(z, p_T) \rightarrow \pi \int \frac{dk_T^2}{k_T^4} f(x_{IP}, k_T^2) \Theta(k_T - p_T). \quad (22)$$

Due to the  $1/k_T^4$  factor, the dominant contribution to the integral comes from the region  $k_T \gtrsim p_T$ . In other words the diffractive production of dijets with transverse momentum  $p_T$  measures the gluons forming the QCD pomeron at  $k_T \approx p_T$  [6]. For  $k_T < p_T$  the exchanged gluon system is unable to resolve the  $q$  and  $\bar{q}$  separately which results in zero net coupling and is reflected by the theta function in (22).

In order to better understand why the contribution for gluon momenta  $k_T < p_T$  vanishes, we divide the integration in (17) into the part corresponding to  $x' > 0$  and the part with  $x' < 0$ . We find from (7) that the condition  $x' > 0$  is fulfilled if the azimuthal angle  $\phi$  between the jet  $\mathbf{p}_T$  and the gluon  $\mathbf{k}_T$  is given by

$$0 < \phi < \alpha \equiv \arccos \left( -\frac{k_T}{2p_T} \right), \quad (23)$$

whereas the region  $\alpha < \phi < \pi$  corresponds to  $x' < 0$ . Notice that if  $k_T \geq 2p_T$  then only the region  $x' > 0$  contributes. For  $k_T < 2p_T$  we split the angular integration in (17) into the positive

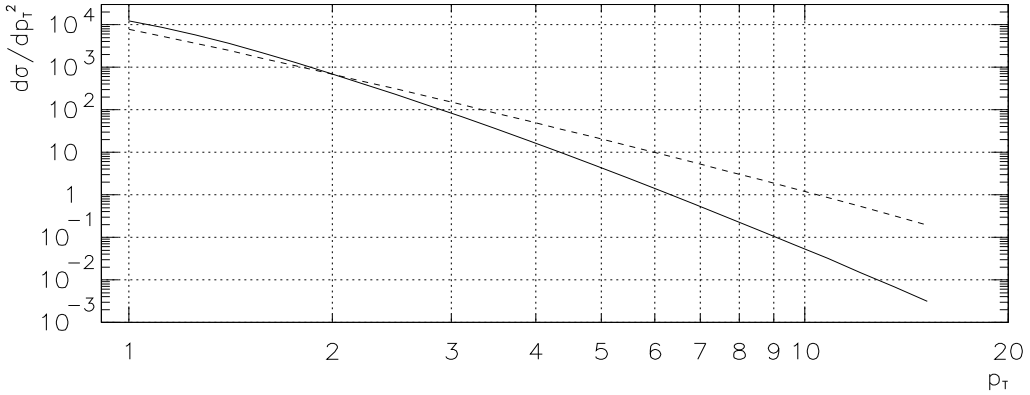


Figure 3: The cross section  $d\sigma/dp_T^2$  as a function of the jet  $p_T$ . The continuous curve shows the cross section with both the regions  $x' > 0$  and  $x' < 0$  included. The dashed curve corresponds to the contribution from the  $x' > 0$  region only, computed with the infrared cut-off  $k_{T0} = 1$  GeV.

and negative  $x'$  parts and carry out the integrations separately

$$\begin{aligned} \phi_1(z, p_T) &= \int \frac{dk_T^2}{k_T^4} \left\{ \int_0^\alpha \dots + \int_\alpha^\pi \dots \right\} = \frac{\pi}{2} \int \frac{dk_T^2}{k_T^4} f(x_{IP}, k_T^2) \\ &\times \left\{ \left[ \frac{1 - \omega^2}{1 + \omega^2} \left( \frac{\alpha}{\pi} \right) - \frac{2 - a}{\sqrt{a^2 - b^2}} \left( \frac{\alpha\beta}{\pi} \right) \right] + \left[ \frac{1 - \omega^2}{1 + \omega^2} \left( 1 - \frac{\alpha}{\pi} \right) - \frac{2 - a}{\sqrt{a^2 - b^2}} \left( 1 - \frac{\alpha\beta}{\pi} \right) \right] \right\}, \end{aligned} \quad (24)$$

where the function  $\beta$  is defined by

$$\beta = \frac{1}{\alpha} \arccos \left( \frac{b + a \cos \alpha}{a + b \cos \alpha} \right). \quad (25)$$

Notice that the sum of the two contributions in the squared brackets, coming from the  $x' > 0$  and  $x' < 0$  regions, simplify in such a way that formula (20) is recovered. In the limiting case when  $\omega = 0$ , the positive and negative  $x'$  parts are equal to  $\alpha(1 - \beta)/\pi$  and  $-\alpha(1 - \beta)/\pi$  respectively, and so their sum gives a vanishing contribution to  $\phi_1$  for  $k_T < p_T$ . As a consequence there is no necessity for an infrared cut-off  $k_{T0}$  on the integration in (20). For  $\omega \neq 0$ , however, the cancellation occurs only between the contributions from the two  $x'$  regions that are linear in  $k_T$ . The first nonzero term is proportional to  $\omega^2 k_T^2$  and leads to a mild logarithmic dependence of  $\phi_1$  on  $k_{T0}$ .

The results of the above analysis are well illustrated by Fig. 2 where the solid lines show the integrand in the curly bracket of (20) and the dotted and dashed lines show, respectively, the  $x' > 0$  and  $x' < 0$  components in (24). Both the cancellation for  $\tau < 1$  and the absence of the  $x' < 0$  component for  $k_T > 2p_T$  are evident. We take  $Q^2 = 0$  and  $p_T = 10$  GeV. The two plots correspond to  $\omega = \bar{Q}/p_T = 0$  and to  $\omega = 0.1$  ( $m_q = 1$  GeV).

It is informative to show the cross section  $d\sigma/dp_T^2$  obtained from (4) for the diffractive photoproduction of dijets in the simplified case when the gluon distribution  $f = 1$  and  $\alpha_S$  is fixed. The prediction is given by the continuous curve in Fig. 3. At large  $p_T$  we anticipate from (22) that  $\phi_1 \sim 1/p_T^2$  and so  $d\sigma/dp_T^2 \sim 1/p_T^6$ . Such behaviour is evident in Fig. 3. Crucial to this behaviour is the cancellation between the  $x' > 0$  and  $x' < 0$  contributions that are linear in  $k_T$ . This is well illustrated by the dashed curve in Fig. 3, which is the cross section which would

have resulted if only the  $x' > 0$  contribution were included. Then  $\phi_1 \sim 1/(p_T k_{T0})$  where  $k_{T0}$  is the infrared cut-off imposed on the  $k_T$  integration. As a result the cross section behaves as  $1/(p_T^4 k_{T0}^2)$  and becomes strongly dependent on the value chosen for the cut-off momentum  $k_{T0}$ . For interest we have extended the predictions in Fig. 3 down to small values of  $p_T$ . The large  $p_T$  asymptotics which we have described above become apparent for  $p_T \gtrsim 4$  GeV.

So far our discussion has been based on the assumption that the gluon distribution in formulae (17) and (18) does not depend on the azimuthal angle. In this case the both  $x'$  regions are weighted by the same value of the gluon distribution  $f(x_{IP})$  when the angular integration in (17) and (18) is performed. As a result we have the delicate cancellation in the region of  $k_T < p_T$ , which we emphasized above. This could be significantly changed when the true off-diagonal gluon distribution  $f(x, x')$  is used, and the two  $x'$  regions are weighted differently during the angular integration. The study of the influence of this effect on the diffractive dijet cross section is a major objective of our analysis.

## 4 Perturbative and nonperturbative contributions

To evaluate the cross sections given in (15) and (16) we have to compute the impact factors  $\phi_1$  and  $\phi_2$  which depend on the off-diagonal gluon distribution. We divide the  $k_T$  integration in (17) and (18) into a nonperturbative and perturbative region according to whether  $k_T$  is smaller or greater than  $k_{T0} \sim 1$  GeV. The angular integration can be performed analytically in the nonperturbative region. For this purpose we analyse the angular dependence of the arguments  $x$ ,  $x'$  and  $x''$  of the gluon distribution function (5) by dividing (7) by  $x_{IP}$  given by (1) and (8)

$$\frac{x'}{x_{IP}} = (1 - z) \left( \frac{\tau^2 + 2\tau \cos \phi}{1 + \omega^2} \right), \quad \frac{x''}{x_{IP}} = z \left( \frac{\tau^2 + 2\tau \cos \phi}{1 + \omega^2} \right). \quad (26)$$

In the nonperturbative region  $\tau = k_T/p_T \ll 1$ , and thus we have

$$|x'|, |x''| \ll x_{IP} \quad \text{and} \quad x \approx x_{IP}. \quad (27)$$

These relations allows us to expand the gluon distribution (5) around the point  $x = x_{IP}$ , i.e. we study  $\tilde{f}$  as function of  $x$  when the value of  $x_{IP}$  is fixed. Thus we obtain

$$\tilde{f}(x, x', k_T^2) \simeq f(x_{IP}, 0, k_T^2) + \left( \frac{\tau^2/2 + \tau \cos \phi}{1 + \omega^2} \right) x_{IP} \frac{\partial f}{\partial x}(x_{IP}, 0, k_T^2). \quad (28)$$

We also expand the expressions in the curly brackets in (17) and (18) in powers of  $\tau$ . Then the angular integration can be performed analytically in the nonperturbative region. The term linear in  $\tau$  vanishes and as a result the first nonzero term is proportional to  $\tau^2$  (that is  $k_T^2$ ). This allows us to express the resulting  $k_T$  integration in terms of the off-diagonal integrated gluon distribution at scale  $k_{T0}^2$  using

$$\int_0^{k_{T0}^2} \frac{dk_T^2}{k_T^2} f(x_{IP}, 0, k_T^2) = G(x_{IP}, 0, k_{T0}^2), \quad (29)$$

$$\int_0^{k_{T0}^2} \frac{dk_T^2}{k_T^2} \frac{\partial f}{\partial x}(x_{IP}, 0, k_T^2) = \frac{\partial G}{\partial x}(x_{IP}, 0, k_{T0}^2). \quad (30)$$

Note that the off-diagonal gluon distribution  $G(x, 0, k^2)$  is not to be identified with the conventional symmetric gluon distribution  $G(x, x, k^2)$  for which the longitudinal fractions are equal and hence the asymmetry variable  $x_{IP} = 0$ .

Thus we finally obtain the following decompositions of the impact factors  $\phi_1$  and  $\phi_2$  into the following nonperturbative and perturbative contributions

$$\begin{aligned}\phi_1(z, p_T) &= \frac{\pi}{p_T^2} \left\{ \frac{2\omega^2}{(1+\omega^2)^3} G(x_{IP}, 0, k_{T0}^2) + \frac{1-\omega^2}{2(1+\omega^2)^3} x_{IP} \frac{\partial G}{\partial x}(x_{IP}, 0, k_{T0}^2) \right\} \\ &+ \int_{k_{T0}^2}^{\infty} \frac{dk_T^2}{k_T^4} \int_0^\pi d\phi \tilde{f}(x, x', k_T^2) \frac{1}{2} \left\{ \frac{1-\omega^2}{1+\omega^2} - \frac{2-a}{a+b \cos \phi} \right\} \end{aligned}\quad (31)$$

and

$$\begin{aligned}\phi_2(z, p_T) &= \frac{\pi}{p_T^2} \left\{ \frac{\omega^2-1}{(1+\omega^2)^3} G(x_{IP}, 0, k_{T0}^2) + \frac{1}{(1+\omega^2)^3} x_{IP} \frac{\partial G}{\partial x}(x_{IP}, 0, k_{T0}^2) \right\} \\ &+ \int_{k_{T0}^2}^{\infty} \frac{dk_T^2}{k_T^4} \int_0^\pi d\phi \tilde{f}(x, x', k_T^2) \left\{ \frac{1}{1+\omega^2} - \frac{1}{a+b \cos \phi} \right\}. \end{aligned}\quad (32)$$

For diffractive dijet production with large  $p_T$  by far the dominant contribution comes from the perturbative region.

Relations (27) are not generally valid in the perturbative region. For example for gluon transverse momenta  $k_T \approx p_T$ , which dominate in the simplified case of Section 3, we find that at least one of the fractions  $|x'|, |x''| \sim x_{IP}$ . For  $z = 1/2$  and  $\omega \ll 1$  this is equivalent to

$$1/2 x_{IP} \lesssim x \lesssim 5/2 x_{IP}. \quad (33)$$

Thus in the perturbative region we study a much broader range of  $x$  of the off-diagonal gluon distributions (5) with the second gluon momentum fractions  $x'$  or  $x''$  being both positive and negative. Also the off-diagonal distributions are required over quite a range of  $k_T$  and are computed using evolution equations. We discuss the off-diagonal evolution in detail in the next section.

## 5 Off-diagonal parton distributions and their evolution

Before discussing the evolution equation for the off-diagonal parton distribution it is convenient to follow Radyushkin [7, 8] and use the notation<sup>3</sup>

$$G_{x_{IP}}(x, k_T) \equiv G(x, x', k_T^2), \quad (34)$$

for the off-diagonal gluon distribution, where the dependence on  $x'$  is implicit through the relation  $x' = x - x_{IP}$ . Both the variables  $x$  and  $x_{IP}$  lie in the interval 0 to 1. Therefore we view the off-diagonal distributions as a family of functions (of  $x$  and the scale  $k_T$ ) labelled by the asymmetry variable  $x_{IP}$ . Radyushkin uses  $\zeta$  for  $x_{IP}$ , but for the moment we will keep the latter notation to indicate that  $x_{IP}$  defined in (1) is the asymmetry variable in the process that we consider.

In the region of  $x > x_{IP}$  (that is  $x' > 0$ ) the off-diagonal gluon distribution  $G_{x_{IP}}(x)$  describes a gluon emitted by the proton with momentum fraction  $x$  together with a gluon absorbed with

---

<sup>3</sup>Alternative notations and formulations of the off-diagonal evolution equations can be found in [3] and [9].

fraction  $x' = x - x_{IP}$ . Thus  $G_{x_{IP}}(x)$  is a generalization of the ordinary diagonal gluon distribution, that is in the diagonal limit  $x_{IP} \equiv x - x' \rightarrow 0$  we have

$$G_{x_{IP}=0}(x) = G(x, x) \equiv x g(x) . \quad (35)$$

We stress once again that we must distinguish between  $G(x, x)$  and  $G_x(x) \equiv G(x, 0)$ . In the first case the asymmetry variable  $x_{IP} = 0$  while in the later  $x_{IP} = x$ .

In the region  $x < x_{IP}$  the second gluon has a *negative* fraction  $x'$  of the proton's momentum. In this case it is more transparent to use  $-k'$  for the momentum of the second gluon, that is we make the replacement

$$k' = x' p + k_T \quad \rightarrow \quad \tilde{k}' = (-k') = |x'| p - k_T . \quad (36)$$

Thus we have the two gluons emitted from the proton with the momenta  $k = xp + k_T$  and  $\tilde{k}'$ . The gluon distribution  $G_{x_{IP}}(x)$  for  $x < x_{IP}$  may be regarded as the probability amplitude for emitting a two gluon colour singlet system from the proton with the individual gluons carrying fractions  $x/x_{IP}$  and  $|x'|/x_{IP}$  of the total momentum of the system  $r = x_{IP}p = k + \tilde{k}'$ .

To evaluate the perturbative contribution we use the full form of the off-diagonal evolution equations for the gluon distribution  $G_{x_{IP}}(x, \mu)$  ( $\mu = k_T$  in our case) and the off-diagonal singlet quark distribution

$$\Sigma_{x_{IP}}(x, \mu) = \sum_{i=1}^{N_f} \{q_{x_{IP}}^i(x, \mu) + \bar{q}_{x_{IP}}^i(x, \mu)\} , \quad (37)$$

where  $q_{x_{IP}}^i$  and  $\bar{q}_{x_{IP}}^i$  are off-diagonal quark and antiquark distributions introduced in analogy to the diagonal case. The evolution equations have the following general form

$$\begin{aligned} \mu \frac{\partial}{\partial \mu} \Sigma_{x_{IP}}(x, \mu) &= \int_0^1 dz P_{x_{IP}}^{QQ}(x, z; \mu) \Sigma_{x_{IP}}(z, \mu) + \int_0^1 dz P_{x_{IP}}^{QG}(x, z; \mu) G_{x_{IP}}(z, \mu) \\ \mu \frac{\partial}{\partial \mu} G_{x_{IP}}(x, \mu) &= \int_0^1 dz P_{x_{IP}}^{GQ}(x, z; \mu) \Sigma_{x_{IP}}(z, \mu) + \int_0^1 dz P_{x_{IP}}^{GG}(x, z; \mu) G_{x_{IP}}(z, \mu), \end{aligned} \quad (38)$$

where the structure of the kernels  $P$  depends on the relations between the  $x, z$  and  $x_{IP}$  variables. The detailed form of the evolution equations extracted from the review [8] is given in the Appendix.

For  $x > x_{IP}$  ( $x' > 0$ ) the integration in (38) covers the range from  $x$  to 1 and the kernels have a form which coincides with the standard Altarelli-Parisi kernels for  $x_{IP} = 0$ . That is (38) reduce to the DGLAP evolution equations [10] in the limit  $x_{IP} = 0$ . On the other hand for  $x < x_{IP}$  ( $x' < 0$ ) the form of the kernels depends on whether the integration variable  $z$  is less or greater than  $x$ . In this case the integration covers the whole range  $(0, 1)$  and in the limit  $x_{IP} = 1$  eqs.(38) reduce to the ERBL evolution equations [4, 5] for the parton distribution amplitudes in a meson.

We solve the evolution equations numerically using an expansion in terms of Chebyshev polynomials and cross-check the solutions against, on the one hand, the known asymptotic solutions of the ERBL equations and, on the other hand, the solutions of the DGLAP evolution equations. Moreover particular attention is paid to the behaviour of the resulting off-diagonal

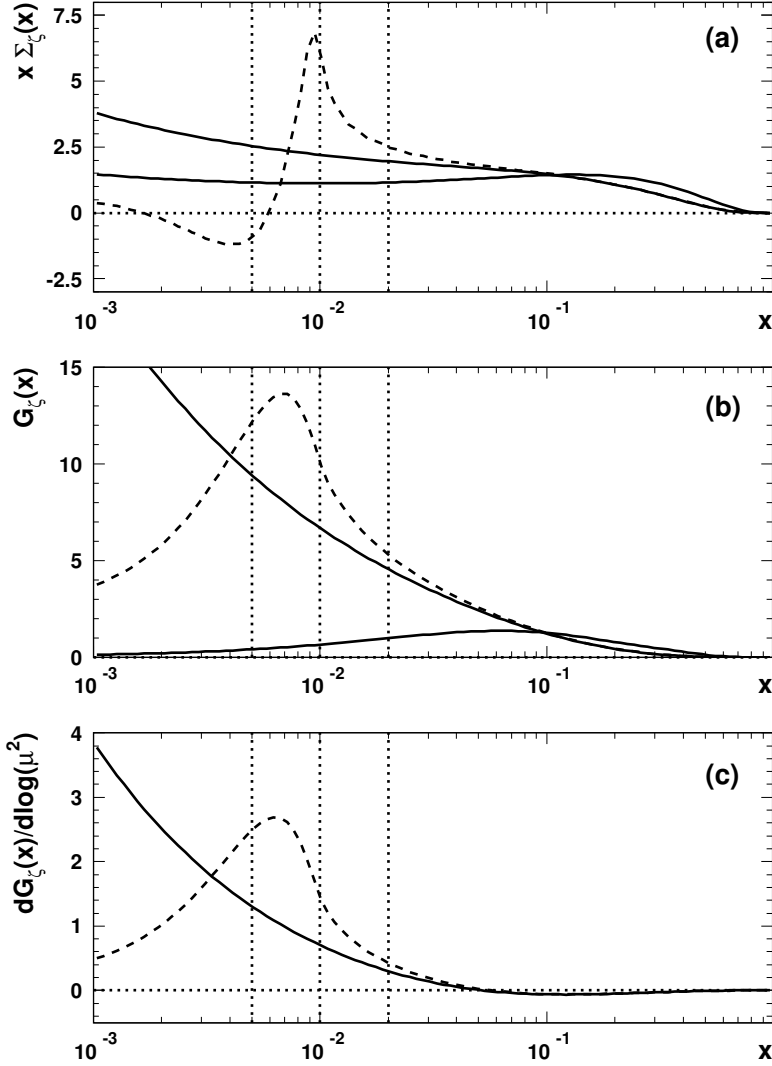


Figure 4: The off-diagonal singlet and gluon distributions and the logarithmic derivative of the gluon distribution (dashed curves) at  $\mu^2 = 10^2$  GeV $^2$  for  $\zeta \equiv x_{IP} = 10^{-2}$  (middle vertical line). The continuous curves show the initial distributions at  $\mu_0^2 = 1$  GeV $^2$  (lower curves) and effect of their evolution using the DGLAP equations (upper curves).

parton distributions at point  $x = x_{IP}$ , where the two (DGLAP-like and ERBL-like) forms of the off-diagonal evolution equations coincide. In all cases we find excellent agreement with the expectations resulting from analytical insight.

In the two upper plots of Fig. 4 we show the off-diagonal singlet and gluon distributions evolved up to  $\mu^2 = 100$  GeV $^2$  (dashed lines) starting from initial conditions specified at  $\mu_0^2 = 1$  GeV $^2$  (lower solid curves). We postulate the following form of the initial distributions

$$\begin{aligned} \Sigma_{x_{IP}}(x) &= (1 - x_{IP})^n \{ (1 - x_{IP}) \Sigma_{MRS}(x) + x_{IP} \Sigma_{BL}(x) \}, \\ G_{x_{IP}}(x) &= (1 - x_{IP})^m \{ (1 - x_{IP}) G_{MRS}(x) + x_{IP} G_{BL}(x) \}, \end{aligned} \tag{39}$$

where  $\Sigma_{MRS}$  and  $G_{MRS}$  are the MRS distributions [11] obtained from global fits based on the DGLAP evolution equations to data for deep inelastic and related hard scattering processes,

and  $\Sigma_{\text{BL}} \sim x(1-x)$  and  $G_{\text{BL}} \sim x^2(1-x)^2$  are asymptotic solutions of the ERBL equations (for the nonsinglet and pure gluon cases). The postulated form in the curly brackets encompasses the basic feature of the off-diagonal parton distributions (and evolution equations) that in the limits  $x_{IP} \rightarrow 0$  or 1 the DGLAP or ERBL components, respectively, are obtained. However in case of a nucleon it is unlikely that the two partons can be *emitted*, sharing the whole nucleon longitudinal momentum (which corresponds to the  $x_{IP} = 1$  limit). This observation is accounted for by the additional powers of  $(1-x_{IP})$  with  $n, m > 0$ . The asymmetry variable was chosen to be  $x_{IP} = 10^{-2}$ , and is indicated by the middle vertical dotted line (the outermost vertical lines correspond to the values  $x_{IP}/2$  and  $2x_{IP}$ ). Clearly the initial distributions are dominated by the DGLAP (MRS) component for such a small value of  $x_{IP}$ . We may compare the dashed curves (the evolved off-diagonal parton distributions) with the upper continuous curves which are obtained from the same initial conditions using the conventional DGLAP evolution equations<sup>4</sup>. The bottom plot compares the logarithmic derivative of  $G_{x_{IP}}(x)$ , which is used in our analysis, see (3), at the same scale  $\mu^2 = 100 \text{ GeV}^2$ . Again the dashed curve corresponds to the off-diagonal case while the continuous curve is obtained using the DGLAP evolution equations.

The solutions reflect the mixed (DGLAP and ERBL) nature of the off-diagonal evolution. This is particularly visible for  $\Sigma_{\zeta=x_{IP}}(x)$  which becomes negative for  $x < x_{IP}$ . This feature is found for the solution of the ERBL evolution equations for the distribution amplitude which is obtained from  $\Sigma_{\zeta}(x)$  in the limit  $\zeta = x_{IP} = 1$ . Thus the off-diagonal parton distributions do not have a probabilistic interpretation, unlike the conventional diagonal distributions. The region  $|x - x_{IP}| \sim x_{IP}$ , indicated by the three vertical lines, is particularly interesting from the point of view of the difference between the off-diagonal and diagonal parton distributions. This region is relevant for gluons with momenta  $k_T \approx p_T$  (see (33)) which are supposed to give an important contribution to the dijet production cross section. We will explore this effect in the next section.

## 6 Effect of off-diagonal distributions on the dijet cross section

For diffractive dijet photoproduction only the cross section (15) for the transversely polarised photons contributes. In addition the  $\phi_2$  part is strongly suppressed for high values of  $p_T$ . Thus we need only analyse the impact factor  $\phi_1$  given by (31). In terms of  $\tau = k_T/p_T$  the perturbative part of  $\phi_1$  has the following form for  $\omega = 0$

$$\phi_1^{(\text{pert})}(z, p_T) = \frac{2\pi}{p_T^2} \int_{\tau_0}^{\infty} d\tau \left[ \frac{1}{\tau^3} \int_0^{\pi} \frac{d\phi}{\pi} \tilde{f}_{x_{IP}}(x, \tau p_T) \frac{1}{2} \left\{ 1 - \frac{1 - \tau^2}{1 + \tau^2 + 2\tau \cos \phi} \right\} \right]. \quad (40)$$

where  $\tau_0 = k_{T0}/p_T$ . The function  $\tilde{f}_{x_{IP}}$  is written in the notation introduced by eq.(34) and is related to the off-diagonal gluon distribution  $G_{x_{IP}}$  through relations (3) and (5). In Fig.5 we show the integrand in the squared brackets in (40) as a function of  $\tau$ . We choose for illustration  $p_T = 5$  and  $10 \text{ GeV}$  for dijet transverse momentum. For each choice we assume the minimum value of  $x_{IP} = 4p_T^2/W^2$ , which corresponds to  $z = 1/2$ .

The results depend subtly on the properties of the gluon distribution  $\tilde{f}_{x_{IP}}$ . Let us start with the simplified case discussed in Section 3. That is we assume that  $\tilde{f}_{x_{IP}} = f_{x_{IP}}(x_{IP}, \tau p_T)$  in (40), hence the gluon distribution does not depend on the azimuthal angle. DGLAP evolution is appropriate in this case and the resulting integrand in (40) is shown by the continuous curves in Fig. 5. The angular integration leads to the step-like form of the integrand which is then

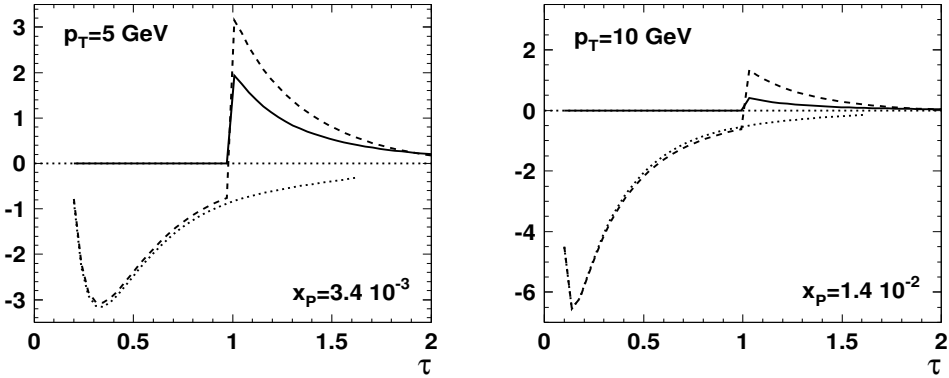


Figure 5: The integrand in the square brackets of (40) for two values of dijet momentum  $p_T$  and the corresponding minimal values of  $x_P$ . The continuous curves show the integrand in the simplified case when  $\tilde{f}_{x_P} = \tilde{f}_{x_P}(x_P)$ , while the dashed curves show the full off-diagonal case  $\tilde{f}_{x_P} = \tilde{f}_{x_P}(x)$ . The dotted lines along the dashed curves show the approximate integrand of (41).

modified by the  $1/\tau^3$  factor to give a function peaked at  $\tau \approx 1$ . This result was anticipated in Section 3.

Now let us explore what happens to the integrand when we use the full off-diagonal gluon distribution  $\tilde{f}_{x_P}(x, \tau p_T)$ , evolved using eqs.(38) from the input given in (39). The results are shown by the dashed curves and are strikingly different from the continuous curves of the simplified case. First we see that for  $\tau \gtrsim 1$  the integrand is larger. This can be easily understood by inspecting the off-diagonal gluon distribution shown in Fig.4c. If  $\tau > 1$  (that is  $k_T > p_T$ ) then during the angular integration the argument  $x$  of the gluon  $\tilde{f}_{x_P}(x)$  spans approximately the region indicated by the outer vertical lines with the gluon following the dashed curves, see also (33). In contrast in the simplified case, the function  $\tilde{f}_{x_P}(x_P)$  is constant as  $x$  spans the allowed range, with its value given by where the solid curve crosses the central vertical line in Fig.4c. The difference in these forms of  $\tilde{f}_{x_P}$  explains why the dashed curve in Fig.5 is larger than the continuous curve for  $\tau \gtrsim 1$ .

The biggest change is in the region  $\tau < 1$ . Recall that in the simplified case the regions of  $x' > 0$  and  $x' < 0$  (to the right and to the left, respectively, of the central vertical line in Fig. 4c) are weighted by the same value  $f_{x_P}(x_P)$  when the angular integration is performed. As a result the terms linear in  $\tau$  coming from the two  $x'$  regions cancel (see Fig. 2 for illustration of this mechanism). However the off-diagonal distributions are asymmetric with respect to the line  $x = x_P$  which divides the two  $x'$  regions (see dashed curve in Fig. 4c). This leads the lack of the above mentioned cancellation and in consequence to an important contribution for  $\tau < 1$ , shown by the dashed lines in Fig. 5. We quantify this observation by expanding the function in the curly brackets in (40) in powers of  $\tau$

$$\phi_1^{(\text{pert})}(\tau < 1) \simeq \frac{2\pi}{p_T^2} \int_{\tau_0}^1 \frac{d\tau}{\tau^3} \int_0^\pi \frac{d\phi}{\pi} \tilde{f}_{x_P}(x, \tau p_T) \left\{ \tau \cos \phi - \tau^2 \cos 2\phi + \dots \right\}. \quad (41)$$

<sup>4</sup>The off-diagonal gluon distribution (Fig.3b) in the  $x' > 0$  region, to the right of the central vertical line, together with the conventional DGLAP curve reproduce the main features of the earlier study of Ref.[2].

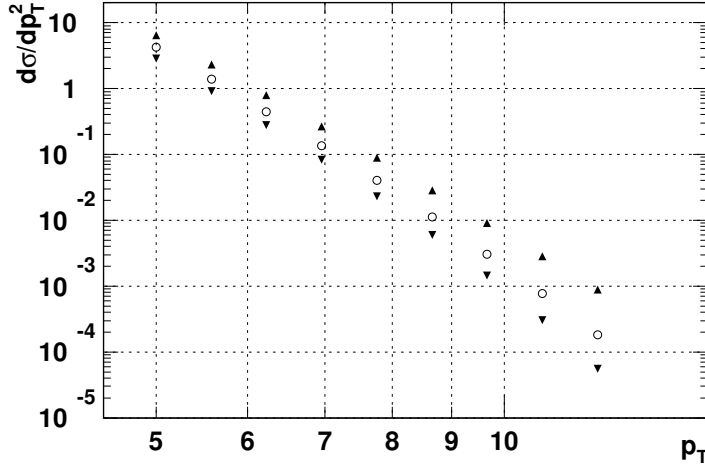


Figure 6: The diffractive dijet photoproduction cross section (in pb/GeV<sup>2</sup>) integrated over the interval  $x_{IP\min} < x_{IP} < 0.05$  as a function of the jet transverse momentum (in GeV). The upper triangular points are obtained in the off-diagonal analysis and the lower ones correspond to the simplified case. The open points are obtained for  $\tilde{f}_{x_{IP}}(x)$  evolved with the DGLAP equations.

Now we retain the term linear in  $\tau$  and perform the angular integration. The resulting integrands are the dotted lines in Fig. 5, extended into the  $\tau > 1$  region to make them visible. Thus in the off-diagonal case the linear in  $\tau$  term from the above expansion does not vanish after the angular integration as it did in the simplified case. Moreover the whole contribution from the  $\tau < 1$  region is essentially determined by this term.

At this point we may worry that the contribution coming from the linear in  $\tau$  term in (41) drastically increases the sensitivity of  $\phi_1^{(\text{pert})}$ , and in consequence the dijet cross section, to the choice of the infrared parameter  $k_{T0}$ . Fortunately this does not happen. The reason is as follows. For  $\tau_0 < \tau \ll 1$  we may additionally expand the function  $\tilde{f}_{x_{IP}}(x)$  in (41) around  $x = x_{IP}$  using formula (28). Then we obtain

$$\begin{aligned} \phi_1^{(\text{pert})}(\tau \ll 1) &\simeq \frac{2\pi}{p_T^2} \int_{\tau_0} d\tau \int_0^\pi \frac{d\phi}{\pi} \left\{ f_{x_{IP}}(x_{IP}, \tau p_T) + \tau \cos \phi \left. \frac{\partial f_{x_{IP}}(x, \tau p_T)}{\partial \ln x} \right|_{x=x_{IP}} \right\} \left\{ \tau \cos \phi \right\} \\ &= \frac{2\pi}{p_T^2} \int_{\tau_0} d\tau \frac{1}{2\tau} \left. \frac{\partial f_{x_{IP}}(x, \tau p_T)}{\partial \ln x} \right|_{x=x_{IP}}, \end{aligned} \quad (42)$$

where the angular integration has been performed to give the final result. Notice that in the simplified case of Section 3 only the first term in the expansion of  $\tilde{f}_{x_{IP}}$  exists and the vanishing contribution is obtained after the angular integration. The full off-diagonal treatment introduces an additional linear in  $\tau$  term which leads to the first nonvanishing contribution being quadratic in  $\tau$ . As a result  $\phi_1^{(\text{pert})}$  still depends at most logarithmically on the parameter  $k_{T0}$ . We have checked that the integrand in (42) reproduces to a good approximation the exact integrand in (40) up to  $\tau \approx 0.3$  for both the values of  $p_T$  chosen for Fig. 5.

The above analysis also shows that the size of the negative contribution to  $\phi_1^{(\text{pert})}$  is mostly determined by the value of logarithmic derivative in  $x$  of  $f_{x_{IP}}(x)$ , taken at the point  $x = x_{IP}$ . In Fig. 4c this derivative corresponds to the slope of the dashed curve at the intersection point with

the middle vertical line. On inspecting Fig.4c notice that the gluon distribution evolved with the DGLAP equations (continuous curve) is also asymmetric with respect to the line  $x = x_{IP}$ . Thus, when such gluon is used in the dijet analysis, a similar negative contribution will be present. The size of this contribution, however, is smaller than in the fully off-diagonal case since the slope of the continuous curve at  $x = x_{IP}$  is always smaller than that of the dashed (off-diagonal) one.

In summary, the off-diagonal parton distributions enhance the contribution to  $\phi_1$  in comparison to the simplified case for  $k_T \geq p_T$  and lead to a significant *negative* contribution in the region  $k_T < p_T$ . Both contributions reflect the particular form of the gluon distribution (3) that is dictated by the off-diagonal evolution equations (38). We have checked that for  $p_T \geq 5$  GeV the net effect after the  $\tau$  ( $k_T$ ) integration in (40) is always negative in the whole range of the  $z$  variable ( $z_{\min} < z < 1/2$ ) in the fully off-diagonal case. Moreover, after squaring and integrating over  $z$  in (15), the impact factor  $\phi_1$  computed using the true off-diagonal distributions leads to a significantly larger cross section for diffractive dijet photoproduction (15) than in the simplified case. In Fig. 6 we show the cross section  $d\sigma/dp_T^2$ , integrated over  $x_{IP}$  between the values  $x_{IP\min} = 4p_T^2/W^2$  and  $x_{IP\max} = 0.05$ . In addition we approximate the effect of the integration over the momentum transfer  $t$  by dividing (15) by the diffractive slope  $A_D = 6$  GeV $^{-2}$ . The upper triangular points correspond to the true off-diagonal result while the lower ones are obtained using the simplified analysis. The open points show the result when  $f_{x_{IP}}(x, k_T)$  is evolved with the DGLAP equations.

We emphasize the special nature of the exclusive diffractive photoproduction of dijets as a probe of the off-diagonal gluon distribution. In our study we have assumed that the cross section is dominated by the QCD subprocess  $\gamma p \rightarrow (q\bar{q})p'$ . A possible contamination may arise from the subprocess  $\gamma p \rightarrow (q\bar{q}g)p'$ , in which the  $q\bar{q}$  pair and the gluon form the two jet system. This background process has been estimated in [12] for inclusive diffractive cross section and found to be important in the region of low  $p_T$  and large diffractive mass  $M$ , but its contribution should be small in our case since we are studying the large  $p_T$  domain.

## 7 Conclusions

The diffractive photoproduction of dijets with high  $p_T$  is an ideal probe of the properties of the off-diagonal (unintegrated) gluon distribution  $f(x, x', k_T^2)$  over a wide kinematic range. Indeed the calculation of the differential cross section  $d\sigma/dp_T^2$  involves the integration over entire range of  $k_T$  with important contributions coming from the region  $k_T \gtrsim p_T$ , and so requires the solutions of the off-diagonal evolution equations to determine  $f$ . Our detailed studies of these equations revealed some novel features. We found that the region  $k_T < p_T$  gives an important contribution to the cross section, originating from the specific properties of the evolved gluon in the  $x' < 0$  (ERBL) and  $x' > 0$  (DGLAP) domains. This is in contrast to the simplified treatment, discussed in Section 3, in which the entire contribution to the cross section comes from the region  $k_T \gtrsim p_T$  leading to a far smaller cross section. In the simplified analysis the gluon distribution was assumed to be only a function of  $x_{IP}$  (and  $k_T^2$ ) – an equivalent approximation was made in the analysis of Ref. [6].

To summarize we found that if the true off-diagonal gluon distribution is used then the impact factor  $\phi_1$  (eq.(31)) receives an important negative contribution from the  $k_T < p_T$  region as well as an enhanced positive contribution from the  $k_T > p_T$  domain. The negative contribution increasingly dominates with growing  $p_T$ . After integration over  $k_T$  the net effect is an overall

enhancement of the dijet cross section in comparison with either the simplified case or with the case in which the conventional DGLAP evolution is used. For example, the enhancement of  $d\sigma/dp_T^2$  at  $p_T = 10$  GeV due to off-diagonal effects is a factor of 3 as compared to using DGLAP evolution, and a factor of 6 compared to the simplified treatment of Section 3 and Ref.[6]. The corresponding factors for jets of  $p_T = 5$  GeV are 1.5 and 2.2 respectively. These enhancements shown in Fig.6. can, in principle, be tested experimentally offering an ideal testing ground of off-diagonal effects.

### Acknowledgements

We thank A. V. Radyushkin, M. G. Ryskin and M. Wüsthoff for valuable discussions. KGB and JK thank, respectively the Royal Society/NATO and the UK Particle Physics and Astronomy Research Council for Fellowships. They also thank the Department of Physics of the University of Durham and Grey College for their warm hospitality. This research has been supported in part the Polish State Committee for Scientific Research grant no. 2 P03B 089 13.

## Appendix

Here we present for reference the full form of the evolution equations for the off-diagonal singlet and gluon distributions  $\Sigma_\zeta(x, \mu)$  and  $G_\zeta(x, \mu)$ , following the prescriptions for the kernels given by Radyushkin in [8]. We use his definitions and notations of off-diagonal (asymmetric in his language) parton distributions. In this notation  $\zeta$  is the asymmetry (skewedness) parameter which in the main body of the paper is equal to the variable  $x_{IP}$

$$\zeta \equiv x - x' = x_{IP} , \quad (43)$$

with  $0 \leq \zeta \leq 1$ . The distributions are defined in such way that in the limit  $\zeta \rightarrow 0$  (the DGLAP limit) we obtain the ordinary *parton distributions*

$$\Sigma_\zeta(x, \mu) \rightarrow \sum_{i=1}^{N_f} \{q^i(x, \mu) + \bar{q}^i(x, \mu)\} \quad (44)$$

$$G_\zeta(x, \mu) \rightarrow x g(x, \mu) . \quad (45)$$

Notice that the ordinary quark distributions are not multiplied by  $x$  as in the gluon case. In the opposite limit  $\zeta \rightarrow 1$  (the ERBL limit) the off-diagonal distributions become the *distribution amplitudes* for finding two partons in a meson sharing fractions  $x$  and  $1 - x$  of its momentum.

$$\Sigma_\zeta(x, \mu) \rightarrow \sum_{i=1}^{N_f} \{\Psi^i(x, \mu) + \bar{\Psi}^i(x, \mu)\} \quad (46)$$

$$G_\zeta(x, \mu) \rightarrow \Psi^g(x, \mu) . \quad (47)$$

Using the notation  $x' = x - \zeta$  and  $z' = z - \zeta$  we have the following equations for  $x > \zeta$  (that is for  $x' > 0$ )

$$\begin{aligned} \mu \frac{\partial}{\partial \mu} \Sigma_\zeta(x, \mu) &= \frac{\alpha_S(\mu)}{\pi} C_F \left\{ \int_x^1 \frac{dz}{x - z} \left[ \left( \frac{x}{z} + \frac{x'}{z'} \right) \Sigma_\zeta(x, \mu) - \left( 1 + \frac{xx'}{zz'} \right) \Sigma_\zeta(z, \mu) \right] \right. \\ &\quad \left. + \Sigma_\zeta(x, \mu) \left[ \frac{3}{2} + \ln \frac{(1-x)^2}{1-\zeta} \right] \right\} \\ &+ \frac{\alpha_S(\mu)}{\pi} N_f \int_x^1 \frac{dz}{zz'} \left[ \left( 1 - \frac{x}{z} \right) \left( 1 - \frac{x'}{z'} \right) + \frac{xx'}{zz'} \right] G_\zeta(z, \mu) , \end{aligned} \quad (48)$$

$$\begin{aligned} \mu \frac{\partial}{\partial \mu} G_\zeta(x, \mu) &= \frac{\alpha_S(\mu)}{\pi} C_F \int_x^1 dz \left[ \left( 1 - \frac{x}{z} \right) \left( 1 - \frac{x'}{z'} \right) + 1 \right] \Sigma_\zeta(z, \mu) \\ &+ \frac{\alpha_S(\mu)}{\pi} N_c \left\{ \int_x^1 dz \left[ \frac{2}{z} \left( 1 + \frac{xx'}{zz'} \right) \left( 1 - \frac{x'}{z'} \right) G_\zeta(z, \mu) \right. \right. \\ &\quad \left. \left. + \frac{[(x/z) + (x'/z')]}{x - z} G_\zeta(x, \mu) - \frac{[(x/z)^2 + (x'/z')^2]}{x - z} G_\zeta(z, \mu) \right] \right\} \\ &+ G_\zeta(x, \mu) \left[ \frac{11 - 2/(3N_f)}{2N_c} + \ln \frac{(1-x)^2}{1-\zeta} \right] , \end{aligned} \quad (49)$$

where  $C_F = 4/3$  and  $N_c = 3$ , and  $N_f$  is the number of active flavours. In the limit  $\zeta = 0$  the above equations become the DGLAP evolution equations.

The equations for  $x < \zeta$  (that is for  $x' < 0$ ) are more complicated since they involve integration with different kernels in the intervals  $(0, x)$  and  $(x, 1)$ . We have

$$\begin{aligned}
\mu \frac{\partial}{\partial \mu} \Sigma_\zeta(x, \mu) &= \frac{\alpha_S(\mu)}{\pi} C_F \left\{ \int_0^x dz \left( \frac{x'}{z'} \right) \left[ \frac{\Sigma_\zeta(z, \mu)}{\zeta} + \frac{\Sigma_\zeta(z, \mu) - \Sigma_\zeta(x, \mu)}{x - z} \right] \right. \\
&\quad + \int_x^1 dz \left( \frac{x}{z} \right) \left[ \frac{\Sigma_\zeta(z, \mu)}{\zeta} + \frac{\Sigma_\zeta(z, \mu) - \Sigma_\zeta(x, \mu)}{z - x} \right] \\
&\quad \left. + \Sigma_\zeta(x, \mu) \left[ \frac{3}{2} + \ln \frac{x(1-x)}{\zeta} \right] \right\} \\
&+ \frac{\alpha_S(\mu)}{\pi} N_f \left\{ \int_0^x \frac{dz}{\zeta^2} \left( \frac{x'}{z'} \right) \left[ 4 \frac{x}{\zeta} + \frac{2x - \zeta}{\zeta - z} \right] G_\zeta(z, \mu) \right. \\
&\quad \left. - \int_x^1 \frac{dz}{\zeta^2} \left( \frac{x}{z} \right) \left[ 4 \left( 1 - \frac{x}{\zeta} \right) + \frac{\zeta - 2x}{z} \right] G_\zeta(z, \mu) \right\} \quad (50)
\end{aligned}$$

$$\begin{aligned}
\mu \frac{\partial}{\partial \mu} G_\zeta(x, \mu) &= \frac{\alpha_S(\mu)}{\pi} C_F \left\{ \int_0^x dz \left( \frac{x'}{z'} \right) \left( 1 - \frac{x}{\zeta} \right) \Sigma_\zeta(z, \mu) + \int_x^1 dz \left( 2 - \frac{x^2}{z\zeta} \right) \Sigma_\zeta(z, \mu) \right\} \\
&+ \frac{\alpha_S(\mu)}{\pi} N_c \left\{ \int_0^x dz \left( \frac{x'}{z'} \right) \left[ \frac{2}{\zeta} \left( 1 - \frac{x}{\zeta} \right) \left( 1 + 2 \frac{x}{\zeta} + \frac{x}{\zeta - z} \right) G_\zeta(z, \mu) \right. \right. \\
&\quad \left. \left. + \frac{(x'/z') G_\zeta(z, \mu) - G_\zeta(x, \mu)}{x - z} \right] \right. \\
&\quad \left. + \int_x^1 dz \left( \frac{x}{z} \right) \left[ \frac{2x}{\zeta^2} \left( 3 - 2 \frac{x}{\zeta} + \frac{\zeta - x}{z} \right) G_\zeta(z, \mu) + \frac{(x/z) G_\zeta(z, \mu) - G_\zeta(x, \mu)}{z - x} \right] \right. \\
&\quad \left. + G_\zeta(x, \mu) \left[ \frac{11 - 2/(3N_f)}{2N_c} + \ln \frac{x(1-x)}{\zeta} \right] \right\}. \quad (51)
\end{aligned}$$

For  $\zeta = 1$  the above equations reduce to the ERBL evolution equations for the distribution amplitudes. It is also instructive to check that both set of equations, that is (48,49) and (50,51), lead to the same limiting set of equations when  $x \rightarrow \zeta$  from both sides.

The four equations (48-51) form a coupled set of equations which, in general, need to be solved simultaneously. However for  $x > \zeta$  it is enough to solve the first two since the right hand side of these equations involves parton distribution for values  $z > x$  (as is true for the DGLAP equations in the limit  $\zeta = 0$ ). This is not the case if  $x < \zeta$ . The solution depends on values of parton distributions in the full interval  $(0, 1)$  and we have to solve all four equations together.

## References

- [1] A. Donnachie and P.V. Landshoff, Phys. Lett. **B285** (1992) 172;  
N.N. Nikolaev and B.G. Zakharov, Z. Phys. **C53** (1992) 331;  
M.G. Ryskin, Z. Phys. **C57** (1993) 89;  
S.J. Brodsky, L. Frankfurt, J.F. Gunion, A.H. Mueller and M. Strikman, Phys. Rev. **D50** (1994) 3134.
- [2] A.D. Martin and M.G. Ryskin, DTP/97/00, hep-ph/9711371, Phys. Rev. **D** (in press).
- [3] L. Frankfurt, A. Freund, V. Guzey and M. Strikman, hep-ph/9703449.
- [4] A.V. Efremov and A.V. Radyushkin, JINR-E2-11535, Dubna, 1978; Phys. Lett **B94** (1980) 245.
- [5] S.J. Brodsky and G.P. Lepage, Phys. Rev. **D22** (1980) 2157.
- [6] N.N. Nikolaev and B.G. Zakharov, Phys. Lett. **B332** (1994) 177.
- [7] A.V. Radyushkin, Phys. Lett. **B380** (1996) 417; Phys. Lett. **B385** (1996) 333.
- [8] A.V. Radyushkin, Phys. Rev. **D56** (1997) 5524.
- [9] X. Ji, Phys. Rev. **D55** (1997) 7114.
- [10] V.N. Gribov, L.N. Lipatov, Sov. J. Nucl. Phys. **15** (1972) 438, 675;  
G. Altarelli, G. Parisi, Nucl. Phys. **B126** (1977) 297;  
Yu.L. Dokshitzer, Sov. Phys. JETP **46** (1977) 641.
- [11] A.D. Martin, W.J. Stirling, R.G. Roberts and R.S. Thorne, DTP/98/10, hep-ph/9803445.
- [12] M. Wüsthoff, Phys. Rev. **D56** (1997) 4311.